Prediction of Dextrose Nucleation Kinetics by the Growth Rate of Crystallites

By *M. Parisi**, *M. Rivallin*, and *A. Chianese*

DOI: 10.1002/ceat.200500350

An investigation on the dextrose nucleation carried out in the presence of seeds is reported. Induction time and nucleation point were measured in seeded solutions by eye and by using a nephelometer. The nucleation point was interpreted as the instant when crystallites, generated by seeds, grow up to crystals of detectable size. By applying the approach proposed by Kashchiev [1], the induction time values obtained were satisfactorily predicted when a birth and spread growth rate model was assumed. Moreover, by extending the same approach to the prediction of the nucleation point, obtained by linear cooling, a nucleation curve in good agreement with the experimental points was determined.

1 Introduction

The α-D-glucose, usually called dextrose, is one of the most widely used sugar compounds in both the food and pharmaceutical industries. It is mainly produced by the hydrolysis of corn starch and crystallized to either anhydrous or monohydrate form. Cooling or evaporative crystallization is usually applied: residence time in the crystallizer is quite high due to the slow growth rate [2]. Crystallization is commonly performed by seeding the feed solution and the secondary nucleation by catalytic mechanism plays an important role in the process performances leading to a large content of fines in the final product.

In spite of the great industrial importance of this product, very few studies on dextrose monohydrate (DX) crystallization kinetics are reported in the literature. In particular, there are few experimental works on the measurement of nucleation point and induction time [3, 4].

This work provides experimental data on both the metastable zone width and the induction time of DX in seeded aqueous solutions. However, the main aim of the work is to show how it is possible to predict the nucleation point of DX aqueous solutions on the basis of the growth rate of crystallites. This was done by applying the approach suggested by Kashchiev [1]. According to this author, the addition of seeds gives rise in the solution bulk to crystallites, with a given number density, which grow until they become crystals of a detectable size. In this case, the nucleation phenomenon is determined by the crystallite growth rate only. This approach was applied to the examined system to first fit the induction time data, then to predict the nucleation curve.

2 Experimental Procedures

The adopted experimental apparatus, shown in Fig. 1, consisted of a 500 cm^3 jacketed glass vessel connected to a thermocryostat bath. The vessel was magnetically stirred at a constant speed of 200 rpm and lighted by a lamp placed behind it in order to visually detect the first appearance of crystals. The measurement was also made by a nephelometric instrument, which detects the nucleation by the sharp increase in light diffusion. A thermocouple was used to measure the solution temperature with an accuracy of $\pm 0.1\,^{\circ}C$.

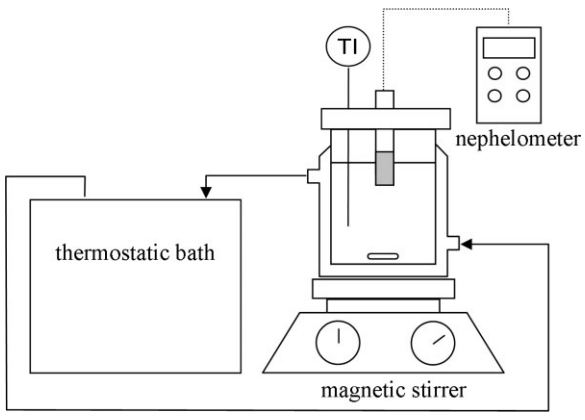

Figure 1. The adopted experimental apparatus.

The DX used was supplied by Roquette Italia. Its purity, measured by HPCL analysis, was 99.4 % b.w. Impurities consisted mainly of maltose and maltotriose derived from a not completed hydrolysis of the starch. The ratio between maltose and maltotriose content was approximately equal to 5.

Two kinds of measurements were made: induction time, at constant temperature, and nucleation point by cooling the solution at a constant rate. When the induction time was measured, the supersaturation was kept constant. Nevertheless, it should be noted that, after preparing the solution at higher temperature, a cooling time was required to reach the fixed supersaturation. Two cooling procedures where adopted.

In a first series of runs, cooling was performed by using the thermocryostat, which allowed a maximum cooling rate of $18\,^{\circ}C/h$. The cooling period of time, in the range from 50 to 90 min, was not negligible when compared with the

[*] M. Parisi (parisi@ingchim.ing.uniroma1.it), M. Rivallin, A. Chianese, Dipartimento di Ingegneria Chimica, Università degli Studi di Roma "La Sapienza", via Eudossiana 18, I-00184 Roma, Italy.

nucleation time. The following experimental procedure was applied. A 70 % b.w. DX solution was prepared by contacting distilled water with an excess of solid and maintaining the slurry in a stirred thermostatted vessel for 24 hours. The solution was then filtered, stabilized at 5 °C above the saturation temperature for one hour and cooled down again to saturation temperature. Seeded and unseeded runs were performed. When seeding was adopted, three to four big crystals were added as soon as equilibrium temperature was reached. The seeding crystals (>425 μm by sieving) were previously washed with saturated ethanol and airdried in order to eliminate the crystals stuck over their surface and to avoid any apparent secondary nucleation when the seeds were poured into solution. The solution was cooled at 18 °C/h down to the fixed temperature corresponding to the desired supersaturation, then the temperature was kept constant until nucleation occurred.

Table 1. Induction times measured at different temperature (W = 70 % b.w.).

Seeded runs					Unseeded runs				
T °C	W_{eq} %	S	t_c s	t_{ind}* s	T °C	W_{eq} %	S	t_c s	t_{ind}* s
25.5	52.5	1.333	4904	120	21.7	49.8	1.406	5665	2820
26.9	53.5	1.308	4622	240	22.5	50.4	1.389	5496	2520
28.9	54.9	1.275	4228	720	23.8	51.3	1.365	5242	2520
30.3	55.9	1.252	3946	1080	23.8	51.3	1.365	5242	1440
31.1	56.5	1.239	3776	1560	23.8	51.3	1.365	5242	1200
34.1	58.6	1.195	3184	3540	25.6	52.6	1.331	4876	1620
					28.9	54.9	1.275	4228	5760

To reduce the cooling time, a different procedure was adopted in a second series of runs. A solution, at a given DX concentration, was prepared at a temperature slightly higher than its saturation point and stabilized in a thermostated vessel, then it was suddenly transferred into the experimental vessel kept at a lower fixed temperature. After this transfer operation, the solution temperature decreased in 2–3 min down to the fixed one. When a constant temperature was reached, 3 to 4 big crystals were added and the run was started. In this series of runs the induction time was always measured at 26 °C, while the concentration of the solution, thus, the supersaturation, varied from run to run.

For the nucleation point measurements the following procedure was adopted. A saturated solution at a fixed temperature was prepared and 3 to 4 big crystals were added. The temperature was then lowered at a constant cooling rate, equal to 10 °C/h, until nucleation occurred.

Since DX crystals are quite fragile and prone to breakage, the presence of fragments generated by the seeded crystals in the examined solutions was carefully checked. During some test runs several samples of solution were withdrawn, observed under a microscope and no fragments were ever observed.

The detection of the nucleation point was accomplished with the naked eye or with a nephelometer recently developed by Chianese et al. [5].

3 Experimental Results

The results of the first series of induction time measurements are summarized in Tab. 1. It should be noted that for all the runs the cooling time, t_c, is longer than or comparable with the measured induction time t_{ind}*, and cannot be neglected. The same results are shown in Fig. 2, where the induction times of the seeded and unseeded runs are compared. The experimental data for the unseeded runs are very scattered, while the seeded runs follow a regular trend. The poor reproducibility of the unseeded run measurements, with deviations higher than 50 % in some cases, is due to the stochastic nature of nucleation in the absence of seeds [6]. Moreover, the seeding strongly decreases the induction time values.

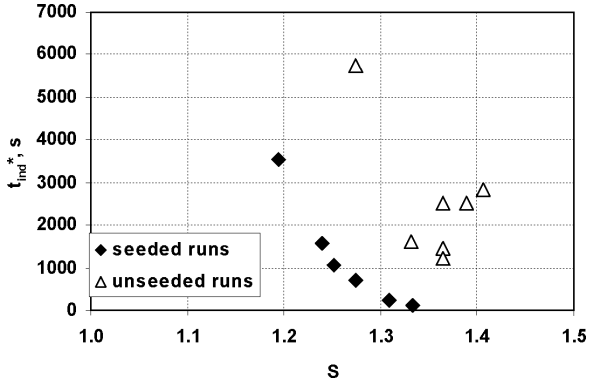

Figure 2. Induction time measured at different temperature (W = 70 % b.w.).

In the second series of runs induction time values, measured at 26 °C, increased from 17 to 316 min for values of supersaturation ratio decreasing from 1.31 to 1.13 (see Tab. 2). The reproducibility of the runs performed at the same operating conditions was acceptable, that is, the time deviation was always within the range of ±10 % of the average value.

The values of the nucleation point by cooling are given in Tab. 3 and Fig. 3, together with the DX solubility curve measured by Parisi et al. [7]. For the investigated DX mass percentages, between 55 and 66 % b.w., nucleation temperatures in the range 13.4 to 30.2 °C were measured. The maxi-

Table 2. Induction times measured at different supersaturation ratio (T = 26 °C).

W %	S	t_{ind} s	W %	S	t_{ind} s	W %	S	t_{ind} s
66.1	1.31	1000	62.2	1.23	3300	58.3	1.16	11560
66.1	1.31	1330	60.9	1.21	6315	58.3	1.16	10590
64.8	1.28	1770	60.9	1.21	5050	58.3	1.16	12780
64.8	1.28	2000	60.9	1.21	5710	57.6	1.14	14190
63.5	1.26	2285	59.6	1.18	8145	57.6	1.14	13360
63.5	1.26	2710	59.6	1.18	7140	57.0	1.13	17700
62.2	1.23	3555	59.6	1.18	7065	57.0	1.13	18980

Table 3. Nucleation point measured at constant cooling rate (dT/dt = 10 °C/h).

W %	T_{eq} °C	T_{nucl} °C	W_{eq} (T_{nucl}) %	S	W %	T_{eq} °C	T_{nucl} °C	W_{eq} (T_{nucl}) %	S
66.1	50.0	29.5	52.7	1.25	60.9	42.0	21.5	47.5	1.28
66.1	50.0	30.2	53.2	1.24	60.9	42.0	22.8	48.4	1.26
63.5	46.0	25.9	50.4	1.26	58.3	38.1	18.3	45.5	1.28
63.5	46.0	26.4	50.7	1.25	58.3	38.1	18.1	45.3	1.29
63.5	46.0	25.6	50.2	1.26	55.0	33.0	13.6	42.4	1.30
63.5	46.0	26.9	51.1	1.24	55.0	33.0	13.4	42.3	1.30

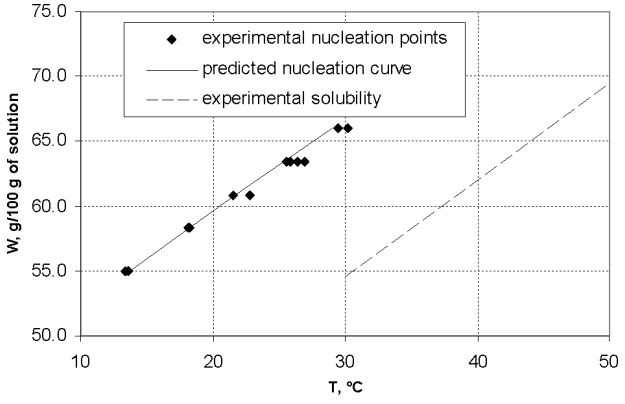

Figure 3. Solubility and nucleation curve of dextrose in water solution (cooling rate: 10 °C/h).

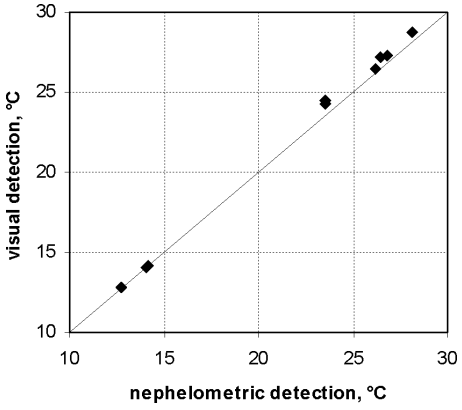

Figure 4. Comparison between nucleation temperatures detected with the naked eye and by a nephelometer.

mum undercooling was almost constant and approximately equal to 20 °C.

Fig. 4 shows the comparison between the visual and the nephelometric temperature measurements. The plot shows good agreement between the two measurement techniques.

4 Discussion

In general, the crystallization induction time, t_{ind}, is considered as the sum of two contributions: the time for the critical nucleus formation, t_n, and the time for its growing up to a detectable size, t_g, that is [8][1)]:

$$t_{ind} = t_n + t_g \quad (1)$$

It is possible to distinguish whether the former or the latter step is the controlling one on the basis of an experimentally assessed dependence of the induction time on the supersaturation [9]. Only if the controlling step is nucleation,

1) List of symbols at the end of the paper.

as is usually the case in homogeneous nucleation, the induction time may be assumed as the time of nucleation and may be expressed as the inverse of the nucleation rate given by the Volmer equation [10]:

$$t_{ind} = A + \exp\left(\frac{\zeta\gamma^3 M^2 N_A f(\phi)}{\rho^2 R^3 T^3 (\ln S)^2}\right) \quad (2)$$

where t_{ind} is the induction time, A an empirical parameter, S the supersaturation, γ the interfacial tension, ζ a shape factor, $f(\phi)$ a function of the wetting angle that is one for homogeneous nucleation and <1 for heterogeneous nucleation, ρ the crystal density, M the molecular density, T the temperature, R the gas constant and N_A the Avogadro number. Eq. (2), written in logarithmic terms, gives:

$$\ln(t_{ind}) = \ln(A) + \frac{\zeta\gamma^3 M^2 N_A f(\phi)}{\rho^2 R^3 T^3 (\ln S)^2} = \ln(A) + B \cdot (\ln S)^{-2} \quad (3)$$

Thus, when Eq. (3) holds, the plot of $\ln(t_{ind})$ vs. $\ln(S)^{-2}$ has a linear trend and any change of the slope B is related to the value assumed by $f(\phi)$, that is to the change of the nucleation mechanism [11].

In the case of seeded crystallization, as soon as the seeds get in contact with the supersaturated solution, an adsorption layer over the seeds surface is set up. The solute molecules in the adsorption layer rearrange themselves firstly as clusters, then as crystal unit cells which are incorporated over the crystal surface. Due to the fluid shear stress, the cluster may be swept away from the crystal surface to the solution bulk, playing a catalytic role with respect to the generation of crystallites in the mother solution. Then, the crystallites grow up until a cloud of crystals of detectable size appears in suspension and the nucleation point is identified. According to this picture, the induction time measured in the seeded experiments performed in this work should mainly be affected by the growth time, t_g. Nevertheless, a first attempt was made to interpolate the experimental data by Eq. (3), by assuming nucleation time as the controlling step. The experimental data were plotted in terms of $\ln(t_{ind})$ vs. $\ln(S)^{-2}$ and the correlation by means of a single straight line was attempted (see Fig. 5). The best fitting of the experimental data was obtained for values of ln(A) and B equal to 6.95 and $4.73 \cdot 10^{-3}$, respectively. The correlation index was quite low, i.e., equal to 0.944.

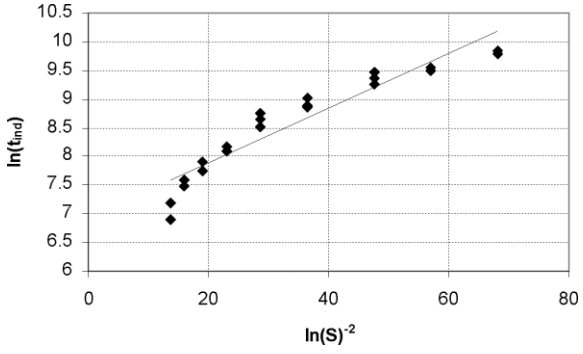

Figure 5. $\ln(t_{ind})$ vs $\ln(S^{-2})$ (T = 26 °C).

The quality of the fitting could strongly improve when the data were fitted by means of two straight lines, the first for the supersaturation range 1.1 to 1.3 and the second one for the range 1.3 to 1.4. The improvement of the fitting may just be a consequence of the increased number of the fitting parameters or may have a physical meaning: the increase of the wetting angle at higher supersaturation. Since this hypothesis has no justification for seeded crystallization runs, there is no physical reason for an interpolation by two different straight lines.

Afterwards, induction time was assumed equal to the time required by the growth of the crystallites in solution up to a detectable crystal size. To predict the induction time values, the approach suggested by Kashchiev [1] was adopted.

If crystallites are present in a supersaturated solution, the induction time is detected when the macroscopic volume of the newly formed solid phase, V_{macro}, reaches a specified fraction α of the overall volume of the system, V. In particular, if the initial crystallite size is much less than the product $t_{ind} \cdot G$, i.e., the crystal detectable size, nucleation occurs when:

$$t_{ind} \cdot G = \left(\frac{\alpha}{2c_m N}\right)^{1/m\nu} = \lambda \quad (4)$$

where N is the crystallite number density, c_m the shape factor, m the dimensionality of growth and ν a constant ranging from 0.5 to 1. For the sake of simplicity, let λ be a coefficient equal to $(\alpha/2c_m N)^{1/m\nu}$ and the induction time as follows:

$$t_{ind} = \frac{\lambda}{G} \quad (5)$$

The analysis of the relationship between the experimental values of t_{ind} and the supersaturation ratio was carried out to determine the most suitable mechanism of growth, as suggested by Kashchiev [1]. Four cases were considered: rough surface growth, spiral growth, birth and spread growth and volume diffusion controlled growth. The best fitting was obtained when the birth and spread growth mechanism was assumed. In this case the linear growth rate may be expressed by the following equation:

$$G = k_{2D} \cdot (S-1)^{2/3} \cdot S^{1/3} \cdot \exp(-B_{2D}/3\ln S) \quad (6)$$

where k_{2D} is a kinetic factor, which is a weak function of S, and:

$$B_{2D} = \frac{\beta\kappa^2 a}{\delta(kT)^2} \quad (7)$$

where β is a numerical 2D shape factor (e.g., π for circle), κ the specific edge-free energy, a the molecular area, δ the number of ions in the formula unit, k the Boltzmann constant. As suggested by Kashchiev [1], the dependence of k_{2D} on S was neglected.

By substituting G given by Eq. (6) into Eq. (5), the following expression for the induction time is derived:

$$t_{ind} = A_S \cdot (S-1)^{-2/3} \cdot S^{-1/3} \cdot \exp(B_{2D}/3\ln S) \quad (8)$$

where $A_S = \lambda/k_{2D}$. In order to interpolate the experimental data by Eq. (8), they were plotted in terms of $\ln(S^{1/3}\text{-}(S-1)^{2/3}t_{ind})$ against $1/\ln(S)$ (see Fig. 6).

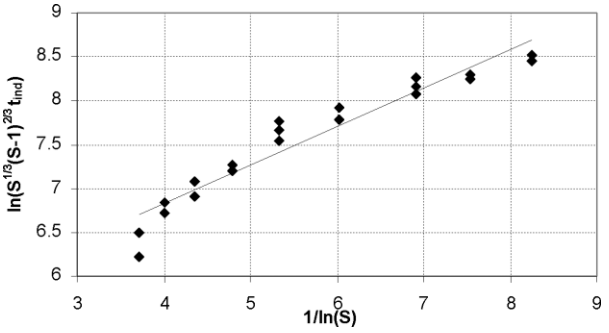

Figure 6. $\ln(S^{1/3}(S-1)^{2/3}t_{ind})$ vs $1/\ln(S)$.

A good fitting was obtained by a straight line with the parameters A_S and B_{2D} equal to 92 s and 1.50, respectively. The correlation index, equal to 0.961, was higher than the value obtained when the Volmer equation was used for data interpolation. Therefore, it may be concluded that, in the case examined, induction time is better modeled by the approach of crystallite growth than by that of spontaneous nucleation in the solution bulk.

The largest deviations between calculated and experimental data were those of the two runs performed at the highest supersaturation, exhibiting the shortest induction times. In this case the transient cooling period of time required for the solution to reach the fixed temperature of 26 °C was not negligible and should be considered as an additional contribution to the induction time.

The adopted approach was, then, extended to predict the nucleation curve, reported in Fig. 3. Throughout each nucleation run the temperature decreased at a constant cooling rate, the solution became more and more supersaturated and the crystallites grew at an increasing rate. It was assumed that the overall volume fraction of the new solid phase corresponding to the nucleation detection, *a*, and the crystallite number density, N, have the same values as those determined for the induction time experiments. As a consequence, the values of *a*, λ, and A_S were also assumed equal in these two kinds of experiments, even though induction time runs were performed at a constant temperature of 26 °C and cooling nucleation runs were carried out at decreasing temperatures in the range 45 to 13 °C. The overall time required to induce nucleation in the cooling experiments, named here t_{nuc}, may be considered as the sum of subsequent contributions, each one corresponding to a different supersaturation value, to the overall induction time. By writing Eq. (8) on the basis of this hypothesis, the condition for the occurrence of nucleation for the polythermal runs can be expressed as:

$$\int_0^{t_{nuc}} (S-1)^{2/3} \cdot S^{1/3} \cdot \exp(-B_{2D}/3\ln S) \cdot dt = A_S \quad (9)$$

where S and B_{2D} are known functions of the temperature, and t_{nuc} is the time corresponding to the nucleation point. The integration at the left hand of Eq. (9) was performed until the value of the integral was equal to A_S. The nucleation point, T_{nuc}, was then derived from the applied linear cooling rate, b = dT/dt, by the simple expression:

$$T_{nucl} = T(t=0) + b\, t_{nuc} \quad (10)$$

Fig. 3 reports the nucleation curve determined by the above-mentioned procedure. Agreement with the experimental data is remarkably good. This successful result shows that the upper limit of the metastable zone width can be referred to the time required to induce nucleation. This-interpretation justifies the enlargement of the metastable zone width which usually occurs at higher cooling rate.

The proposed approach was also applied to the seeded runs of the first series of induction time measurements: in this case the cooling time, t_c, cannot be neglected and the induction time can be predicted by the following equation:

$$\int_0^{t_c} (S-1)^{2/3} \cdot S^{1/3} \cdot \exp(-B_{2D}/3\ln S) \cdot dt + (S-1)^{2/3} \cdot S^{1/3} \cdot \exp(-B_{2D}/3\ln S)\Big|_{T_c} \cdot t^*_{ind} = A_S \quad (11)$$

where T_c is the constant temperature reached after the cooling time t_c. The obtained results are shown in Fig. 7. Once more, agreement between the experimental values and the predicted curve is satisfactory. The maximum discrepancy between experimental and calculated values is less than 7 % of the overall run time.

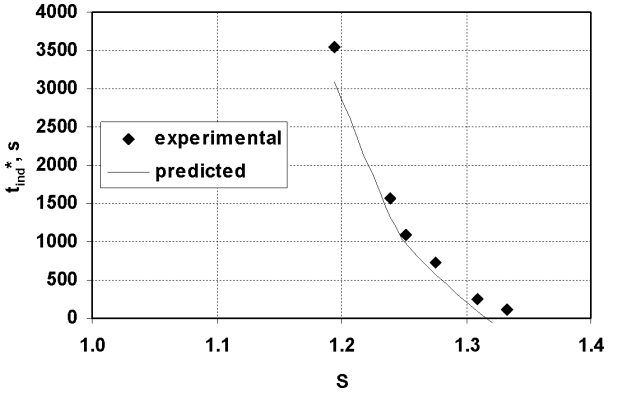

Figure 7. Experimental and predicted induction time for the 1st series of runs.

5 Conclusion

In this work, nucleation for seeded crystallization runs of dextrose monohydrate in aqueous solutions was interpreted in the light of the Kashchiev approach. Both induction time and nucleation point were considered to be determined by the growth rate of crystallites, present in solution because of seeding, which gives rise to a well-defined volume fraction of solids in suspension.

After the performance of two series of experiments, the induction time values were used to determine the kinetic coefficients of the crystallite growth rate, then, a procedure was developed to predict the nucleation curve. A remarkably good comparison between the estimated and experimental values of nucleation point was obtained.

Further confirmations of the suggested procedure with reference to other crystallization systems are required, however, the approach proposed here appears very promising to predict the metastable zone width for seeded experiments.

Acknowledgement

This work was done in the framework of the European Project Sinc-Pro (contract no. G1RD-CT-2002–00756). The authors gratefully acknowledge the grant received by the European Community.

Received: November 11, 2005

Symbols used

a	[m^2]	molecular area
A_S	[s]	coefficient equal to λ/k_{2D}
b	[$°C\,s^{-1}$]	cooling rate
B_{2D}	[–]	coefficient defined by Eq. (7)
c_m	[–]	shape factor
G	[$m\,s^{-1}$]	linear growth rate
k	[$J\,K^{-1}$]	Boltzmann constant
k_{2D}	[$m\,s^{-1}$]	kinetic factor in the growth rate expression
m	[–]	dimensionality of crystallites growth
M	[$kg{\cdot}mol^{-1}$]	molecular density
N	[m^{-3}]	crystallites density
N_A	[mol^{-1}]	Avogadro number
R	[$J\,mol^{-1}K^{-1}$]	gas constant
S	[–]	supersaturation ratio
t	[s]	time
t_c	[s]	cooling time
t_{ind}	[s]	induction time
t_{nucl}	[s]	nucleation time
T	[K or °C]	temperature
T_{nucl}	[K or °C]	nucleation temperature
W	[–]	mass percentage, kg of anhydrous dextrose/100 kg of solution

Greek symbols

α	[–]	volume fraction of visible nuclei
β	[–]	2D shape factor
γ	[$J\,m^{-2}$]	interfacial tension
δ	[–]	number of ions in the formula unit
κ	[$J\,m^{-1}$]	specific edge free energy
λ	[m]	coefficient in Eq. (4) equal to $t_{ind}{\cdot}G$
ν	[–]	constant in Eq. (4)
ρ	[$kg\,m^{-3}$]	crystal density
ϕ	[rad]	wetting angle
ζ	[–]	shape factor in Volmer equation

References

[1] M. C. van der Leeden, D. Verdoes, D. Kashchiev, G. M. van Rosmalen, in *Advances in Industrial Crystallization* (Eds: J. Garside, R. J. Davey, A. G. Jones), Butterworth-Heinemann Ldt, Oxford **1991**.
[2] Kirck-Othmer, *Encyclopaedia of Chemistry and Technology,* 4th ed., John Wiley & Sons, New York **1997**.
[3] E. G. Bondar V. V. Petrushevskij, *Sakh. Prom-st* **1968**, *42 (7)*, 60.
[4] N. G. Gulyuk, *Sakh. Prom-st* **1980**, *11*, 43.
[5] A. Chianese, M. Bravi, A. Mascioletti, *Italian Patent RM A000182*, **2005**.
[6] A. F. Izmailov, A. S. Myerson, S. Arnold, *J. Cryst. Growth* **1999**, *196*, 234.
[7] M. Parisi, I. M. Hernàndez, A. Chianese, *presented at CGOM6*, Glasgow **2003**.
[8] D. Kashchiev, G. M. Van Rosmalen, *Cryst. Res. Technol.* **2003**, *38*, 555.
[9] O. Söhnel, J. W. Mullin, *J. Colloid Interface Sci.* **1988**, *123*, 43.
[10] M. Volmer, *Kinetic der Phasenbildung*, Butterworths, London **1939**.
[11] O. Söhnel, J. Garside, *Precipitation*, Butterworth-Heinemann, Oxford **1992**.

